The Local Reaction Rate in Round-Jet Diffusion Flames*

Kaoru FURUSHIMA**, Yukio KAWANO***,
Kazuhiro AOYAMA**** and Yoshiaki ONUMA*****

A combustion model for turbulent diffusion flames is estimated frequently through the comparison of the simulated result with the experimental one. Usually, profiles of time-averaged concentration and temperature are used in that comparison, because the local reaction rate cannot be directly measured. However, since their profiles are also influenced largely by transport phenomena, it is difficult to estimate the combustion model properly with this method. Therefore, it is desirable to calculate the local reaction rate from experimental results and compare it with the simulated one. In the present study, from this point of view, the local reaction rate was tried to obtain by numerical calculation using measured values for a hydrogen jet diffusion flame. Then, it was suggested through the comparison of the obtained result with the simulated one that the method proposed here can provide reliable values for the local reaction rate.

Key Words: Combustion, Diffusion Combustion, Numerical Analysis, Reaction Rate, Effective Diffusion Coefficient, Combustion Model, Modeling

1. Introduction

Many problems remain to be solved in the modeling of turbulent combustion. In the field of fluid dynamics, the development of direct numerical simulation which does not need a model is rapidly progressing, as following the advancement of computer performance. In dealing with the turbulent combustion field, however, it is supposed that some models are necessary for the simulation even in the future.

The modeling of reaction rates may be most important in the simulation. The combustion model for turbulent diffusion flames is evaluated frequently by the comparison of simulation results with experimental ones. Usually, profiles of time-averaged concentration and temperature are used in that comparison, because local reaction rates cannot be measured directly. However, since their profiles are also influenced largely by transport phenomena, it is difficult to estimate the combustion model properly with this method. Therefore, it is desirable to calculate local reaction rates from experimental results and compare them with simulated ones.

Senecal et al.[1),(2)] developed a method to calculate numerically local reaction rates and effective diffusion coefficients using experimental results for a ducted, axi-symmetric, turbulent diffusion flame of propane and air. In the present study, we improved their method of measurement and numerical calculation and tried to obtain more accurately their values for a hydrogen jet diffusion flame. Simultaneously, we simulated numerically that flame and compared the simulated local reaction rates and the diffusion coefficients with the foregoing experimental ones.

* Received 14th August, 1995. Japanese original: Trans. Jpn. Soc. Mech. Eng., Vol. 60, No. 579, B(1994), pp. 3951-3956 (Received 22nd November, 1993)

** Mechanical and Electrical Engineering, Yatsushiro National College of Technology, 2627 Hirayama-Shinmachi, Yatsushiro 866, Japan

*** Mechanical Engineering, Miyakonojou National College of Technology, 473-1, Yoshio-machi, Miyakonojou 885, Japan

**** Nippon Sanso, 4-320, Sachiku-Tsukahori, Kawasaki 210, Japan

***** Mechanical Engineering, Toyohashi University of Technology, Azahibarigaoka-Tenpaku-cho, Toyohashi 441, Japan

Nomenclature

C_{g1}, C_{g2} : empirical constants appearing in the g equation
C_1, C_2, C_D : empirical constants appearing in the k-ε turbulence model
D_{eff} : effective diffusion coefficient
f : mixture fraction
g : square of the fluctuation of mixture fraction
k : turbulence kinetic energy
m_i : mass fraction of species i
R_i : reaction rate of species i
r : radial distance from the axis of symmetry
$\bar{U}$, $\tilde{U}$: time-averaged velocity in the stream-wise direction
$\bar{V}$, $\tilde{V}$: time-averaged velocity in the radial direction
x : distance in the stream-wise direction from nozzle tip
ε : dissipation rate of turbulent kinetic energy
μ_l : viscosity
μ_t : turbulent viscosity
ρ : density
σ_k, σ_ε : turbulent Prandtl number
σ_f, σ_g, σ_i : turbulent Schmidt number
Capped symbol
— : conventional time average (Reynolds average)
~ : density-weighted average (Favre average)

2. Experimental Apparatus and Procedure

A turbulent diffusion flame was formed with a fuel gas jet issuing vertically upward from a circular nozzle. A mixture of hydrogen and nitrogen (volumetric ratio of H_2 to N_2: 1/2) was used as fuel. Inside diameter of the fuel nozzle is 6 mm and the fuel was fed at 25 m/s through it. Surrounding air issues parallel to the fuel jet at 3 m/s from a coaxial orifice of 140 mm inside diameter.

Time-averaged and rms fluctuating velocity, chemical species concentrations and temperature were measured with a laser doppler velocimeter, gas chromatography and thermocouple, respectively. To obtain accurate concentrations, we improved a gas chromatography so as to measure all stable species, such as H_2, O_2, H_2O and N_2, at the same time. Since the concentration of H_2O plays an important role in this study, we paid special attention to the measurement of H_2O concentration. For example, a gas sampling line and a gas chromatography were warmed up sufficiently to prevent the water vapor from condensing.

3. Calculation Method of Local Reaction Rates

If it is assumed that effective diffusion coefficients are the same for all chemical species, the conservation equation of species i for the axi-symmetric jet diffusion flame is:

$$\bar{\rho}\tilde{U}\frac{\partial \tilde{m}_i}{\partial x}+\bar{\rho}\tilde{V}\frac{\partial \tilde{m}_i}{\partial r}=\frac{1}{r}\frac{\partial}{\partial r}\left(\bar{\rho}D_{eff}r\frac{\partial \tilde{m}_i}{\partial r}\right)+\bar{R}_i \quad (1)$$

Since no element is produced in the chemical reaction, the conservation equation of hydrogen elements is:

$$\bar{\rho}\tilde{U}\frac{\partial \tilde{m}_H}{\partial x}+\bar{\rho}\tilde{V}\frac{\partial \tilde{m}_H}{\partial r}=\frac{1}{r}\frac{\partial}{\partial r}\left(\bar{\rho}D_{eff}r\frac{\partial \tilde{m}_H}{\partial r}\right) \quad (2)$$

Equation (3) is given by integrating Eq. (2) from a symmetry axis to an arbitrary streamline r_s. Then, effective diffusion coefficients D_{eff} are obtained through substituting experimental data into Eq. (3); that is, the element H is used as a tracer in this calculation.

$$\frac{\partial}{\partial x}\int_0^{r_s}\bar{\rho}\tilde{U}r\tilde{m}_H dr=\left[\bar{\rho}D_{eff}r\frac{\partial \tilde{m}_H}{\partial r}\right]_{r=r_s} \quad (3)$$

Equation (4) is given from Eq. (1) with the same operation as in Eq. (3). Local reaction rates are obtained through substituting the above D_{eff} and experimental data into Eq. (4)[1],[2].

$$\frac{\partial}{\partial x}\int_0^{r_s}\bar{\rho}\tilde{U}r\tilde{m}_i dr-\left[\bar{\rho}D_{eff}r\frac{\partial \tilde{m}_i}{\partial r}\right]_{r=r_s}=\int_0^{r_s}\bar{R}_i r dr \quad (4)$$

Before we substitute experimental data into the above equations, the data were smoothed in the radial direction with "smoothed spline function" fitting. And when we needed the interpolation of data in the progress of the numerical calculation, we used "spline function" fitting. This calculation method is named hereafter "Method A" for the convenience of description.

Time-averaged velocity measured with a laser doppler velocimeter is considered conventional time-average (Reynolds average) $\bar{U}$, because a tracker type signal analyzer was used. Chemical species concentrations measured with a gas chromatography are approximately density-weighted average (Favre average) $\tilde{m}_i$. Temperature measured with a thermocouple may indicate an intermediate value between the two kinds of average. Then, the present experiment cannot give the correct values for $\tilde{U}$ and $\bar{\rho}$, which are a function of $\tilde{m}_i$ and $\tilde{T}$, in Eqs. (3) and (4). In the numerical calculation, the measured, conventional time-averaged $\bar{U}$ was used instead of the density-weighted average, $\tilde{U}$, and the measured concentration and temperature were taken to be conventional time-averaged values in the calculation of $\bar{\rho}$. Though it has been reported[3] that the differences between $\bar{U}$ and $\tilde{U}$, and $\bar{T}$ and $\tilde{T}$ are small in the flame of comparatively weak turbulence, it is difficult to estimate the amount of error caused by the above approximation.

4. Modeling

The basic equations consist of the Favre-averaged conservation equations of mass, momentum and scalar, to which boundary layer approximation was applied. The mixture fraction f, defined by Eqs.(5) and(6), was used as the scalar in connection with a combustion model,

$$\phi = S m_{H_2} - m_{O_2} \tag{5}$$

$$f = \frac{\phi - \phi_\infty}{\phi_0 - \phi_\infty} \tag{6}$$

where m_{H_2} and m_{O_2} are mass fractions of H_2 and O_2, S is stoichiometric oxygen-hydrogen mass ratio, and ϕ_0 and ϕ_∞ are the ϕ values of nozzle fluid and surrounding air. Concentration of chemical species, temperature and gas density were calculated from f on the assumption that effective diffusion coefficients are the same for all chemical species and heat.

In a combustion model, one-step irreversible reaction with fast chemistry was assumed and the probability density function(PDF)was introduced for mixture fraction to consider turbulent mixing. A clipped Gaussian distribution was used as PDF, and form of PDF at local position was specified in terms of the mean $\tilde{f}$ and variance g of f, obtained from Eqs.(7) and(8). The same method as in Ref.(4)was applied to the numerical calculation.

$$\bar{\rho}\tilde{U}\frac{\partial \tilde{f}}{\partial x} + \bar{\rho}\tilde{V}\frac{\partial \tilde{f}}{\partial r} = \frac{1}{r}\frac{\partial}{\partial r}\left(r\frac{\mu_{eff}}{\sigma_f}\frac{\partial \tilde{f}}{\partial r}\right) \tag{7}$$

$$\bar{\rho}\tilde{U}\frac{\partial g}{\partial x} + \bar{\rho}\tilde{V}\frac{\partial g}{\partial r} = \frac{1}{r}\frac{\partial}{\partial r}\left(r\frac{\mu_{eff}}{\sigma_g}\frac{\partial g}{\partial r}\right) + C_{g1}\mu_t\left(\frac{\partial \tilde{f}}{\partial r}\right)^2 - C_{g2}\bar{\rho}\frac{g\varepsilon}{k} \tag{8}$$

The k-ε two-equation model represented in Eqs.(9) ~(11)was used as a turbulence model.

$$\bar{\rho}\tilde{U}\frac{\partial k}{\partial x} + \bar{\rho}\tilde{V}\frac{\partial k}{\partial r} = \frac{1}{r}\frac{\partial}{\partial r}\left\{r\left(\mu_l + \frac{\mu_t}{\sigma_k}\right)\frac{\partial k}{\partial r}\right\} + \mu_t\left(\frac{\partial \tilde{U}}{\partial r}\right)^2 - \bar{\rho}\varepsilon \tag{9}$$

$$\bar{\rho}\tilde{U}\frac{\partial \varepsilon}{\partial x} + \bar{\rho}\tilde{V}\frac{\partial \varepsilon}{\partial r} = \frac{1}{r}\frac{\partial}{\partial r}\left\{r\left(\mu_l + \frac{\mu_t}{\sigma_\varepsilon}\right)\frac{\partial \varepsilon}{\partial r}\right\} + C_1\frac{\varepsilon}{k}\mu_t\left(\frac{\partial \tilde{U}}{\partial r}\right)^2 - C_2\bar{\rho}\frac{\varepsilon^2}{k} \tag{10}$$

$$\mu_t = C_D\bar{\rho}\frac{k^2}{\varepsilon} \tag{11}$$

The constants in Eqs.(7)~(11)were assigned the following values which are in general use.

$\sigma_k = 1.0$ $\sigma_\varepsilon = 1.3$ $\sigma_f, \sigma_g = 0.7$
$C_D = 0.09$ $C_1 = 1.44$ $C_2 = 1.92$
$C_{g1} = 2.8$ $C_{g2} = 1.92$

Local reaction rates were derived by substituting calculated results into Eq.(12), which is given from Eq.(1), because they were not obtained directly in the model described above. Effective diffusion

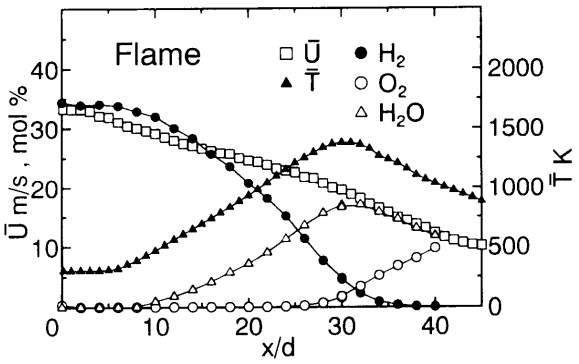

(a) Experimental results

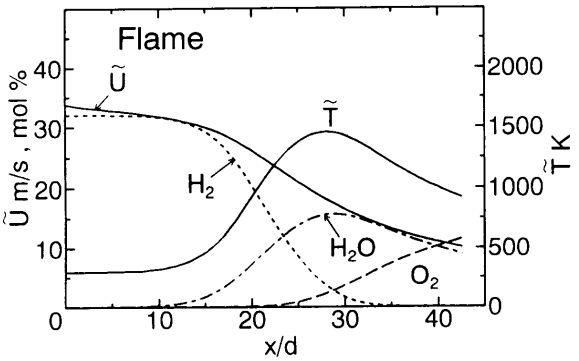

(b) Simulation results

Fig. 1 Axial profiles of velocity, temperature and concentration along symmetry axis

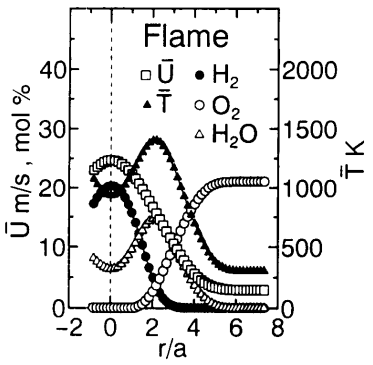

(a) Experimental results

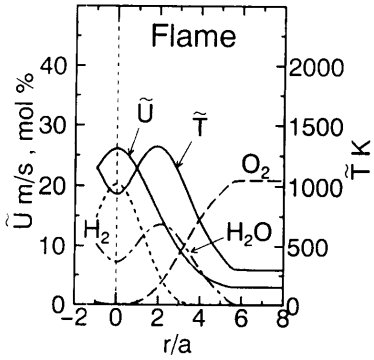

(b) Simulation results

Fig. 2 Radial profiles of velocity, temperature and concentrations on the cross section of $x/d = 20$

coefficients were provided with $D_{eff}=\mu_{eff}/(\sigma_i\bar{\rho})$. This calculation method for local reaction rates and effective diffusion coefficients is named "Method B" hereafter.

$$\int_0^{r_s}\bar{R}_i r dr=\int_0^{r_s}\bar{\rho}\tilde{U}\frac{\partial\tilde{m}_i}{\partial x}r dr+\int_0^{r_s}\bar{\rho}\tilde{V}\frac{\partial\tilde{m}_i}{\partial r}r dr-\left[\bar{\rho}D_{eff}r\frac{\partial\tilde{m}_i}{\partial r}\right]_{r=r_s} \quad (12)$$

5. Results and Discussion

5.1 Experimental and calculated results

Measurements were carried out along the axis of symmetry and on the cross sections of $x/d=10$, 15, 20, 25, 30 and 35. As an example, Figs. 1(a) and 2(a) show the axial profiles and the radial ones on $x/d=10$ cross section, respectively. x is the distance from the nozzle tip and r is the radial distance from the axis of symmetry; d and a are the inside diameter and radius of the nozzle; $\bar{U}$ and $\bar{T}$ are time-averaged axially-directed velocity and temperature. Almost all experimental data are observed to be on smooth curves.

Figures 1(b) and 2(b) are the simulated results corresponding to the experimental results shown in Figs. 1(a) and 2(a). Though the predicted results agree with the experimental ones in the axial profiles. Particularly, the reduction rate of H_2 concentration, which plays an important role in the calculation of local reaction rates, was underestimated in the upstream region, and overestimated in the downstream. Judging from the disappearance positions of H_2 and the peak positions of temperature, the predicted flame length is found to be shorter by about 4 in x/d than actual one.

5.2 Examination of Method A

Before effective diffusion coefficients D_{eff} and local reaction rates $\bar{R}_{H_2}$ are calculated from experimental results, the accuracy of Method A was examined by calculating those values with the same method using the simulated results such as shown in Figs. 1(b) and 2(b). The data on the eleven cross sections from $x/d=10$ to 35 were used in the calculation.

Figure 3 shows the radial profiles of two kinds of D_{eff}. The plots are the D_{eff} values obtained with Method A, which is indicated "D_A" hereafter. The lines show the values of $D_{eff}=\mu_t/(\sigma_t\cdot\bar{\rho})$ obtained with Method B, which is indicated "D_B" hereafter. Figure 3(a) shows the results for the flame. "D_A" agrees well with "D_B" in almost all area, though some discrepancy is observed around the symmetry axis. Since the numerical simulation is conducted using "D_B" as diffusion coefficients and "D_A" is derived from the simulation results, D_A should coincide with D_B. The

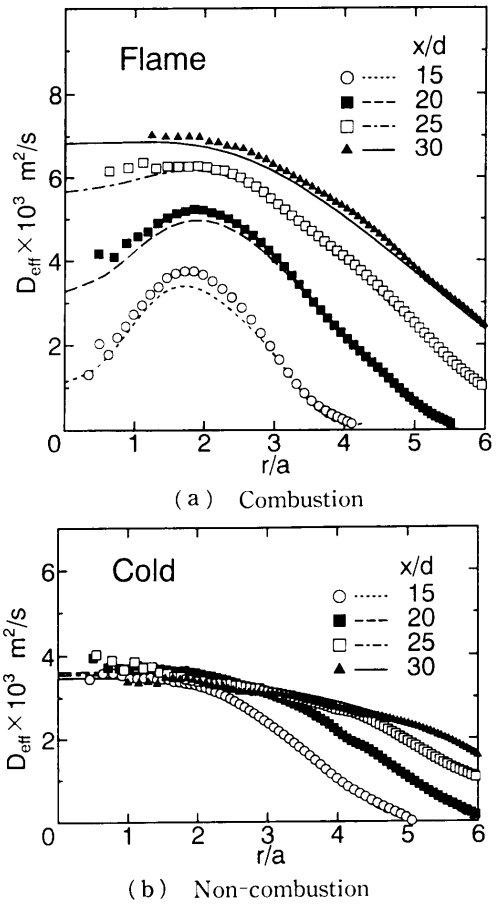

Fig. 3 Radial profiles of effective diffusion coefficient on the cross section. Symbols indicate axial position in x/d. They are demonstration to examine the accuracy of calculation program. Plot and line are obtained from Method A and Method B, respectively.

reason why perfect agreement was not achieved is considered as follows; that is, D_A was calculated using fitting curves connecting simulated data points of rough interval, and the gradient of the curve has a large effect on the results. Particularly, the discrepancy around the symmetry axis becomes larger because the gradient of concentration profiles is small there. Figure 3(b) shows the results for the H_2/N_2 mixture jet without combustion. Though a little discrepancy is also seen in the central region like in the flame, the agreement is good.

Figure 4 shows the radial profiles of local reaction rates R_{H_2}. The plot indicates the result of Method A, and the line indicates the results of Method B. Both results show good agreement also in the local reaction rates.

From Figs. 3 and 4, it can be concluded that Method A can give accurate effective diffusion coefficients and local reaction rates except for a central region, if reliable values are used as source data.

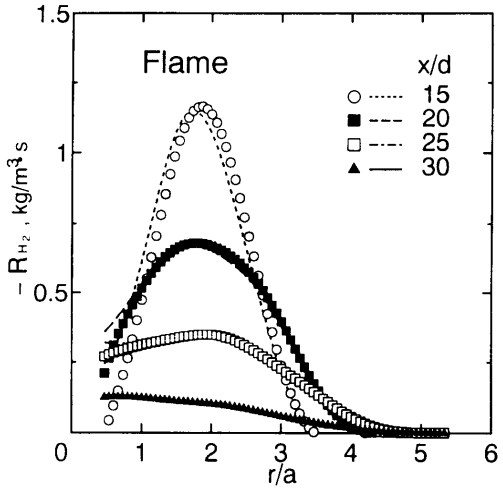

Fig. 4 Radial profiles of local reaction rate of H_2 on the cross section. Symbols indicate axial position in x/d. They are demonstration as well as Figs. 3.

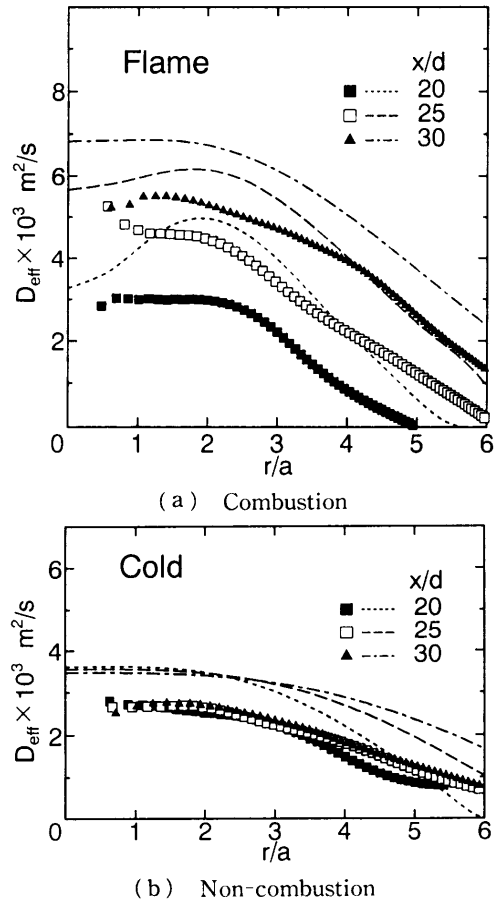

(a) Combustion

(b) Non-combustion

Fig. 5 Radial profiles of effective diffusion coefficient on the cross section. Symbols indicate axial position in x/d. Plot is conducted with the experimental data by using Method A and line shows the simulation results.

5.3 Local reaction rates and diffusion coefficients

Next, effective diffusion coefficients and local reaction rates were calculated using the experimental data, and compared with the simulated results.

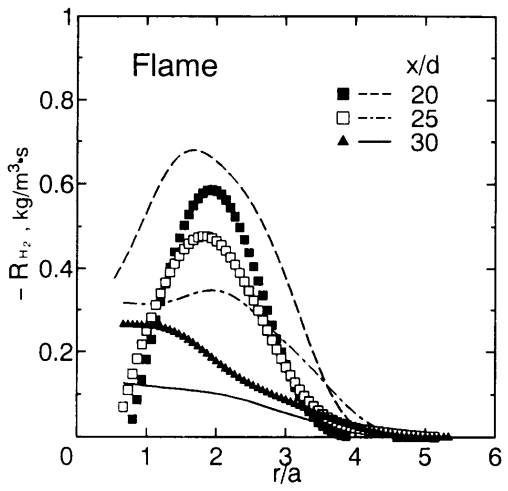

Fig. 6 Radial profiles of local reaction rate of H_2 on the cross section. Symbols indicate axial position in x/d. Plot is conducted with the experimental data by using Method A and line shows the simulation results.

Figures 5(a) and (b) show the radial profiles of D_{eff} for the cases of combustion and non-combustion, respectively. The plots are the results obtained from the experimental data with Method A, and the lines are the simulated results shown in Fig. 3(a). The experimental data on the six cross sections from x/d =10 to 35 were used in the calculation of Method A. Comparing two kinds of the results, though some discrepancy is seen in the detail and the absolute value, both results may show good correspondence in the shape of the radial profile, in the change of the shape with the axial distance, in the difference between the profiles for combustion and non-combustion and in the trend that the value becomes larger as going downstream.

Figure 6 shows the radial profiles of local reaction rates obtained from the experimental data with the simulated ones. Both results show good agreement in the shape of the radial profile and the changing manner of the shape with the axial distance. But, comparing them in the corresponding cross sections, the agreement does not appear so good. The simulated reaction rates are larger than the experimental ones on x/d=30. These discrepancies were caused by the deficient prediction for the axial profile of H_2 concentration, as described before in Fig. 1(b).

Figure 7 shows the correlation among the profiles of local reaction rates and concentration of three chemical species on the cross section of x/d=20. The plots and the lines indicate the experimental and the simulated results, respectively. Comparing both

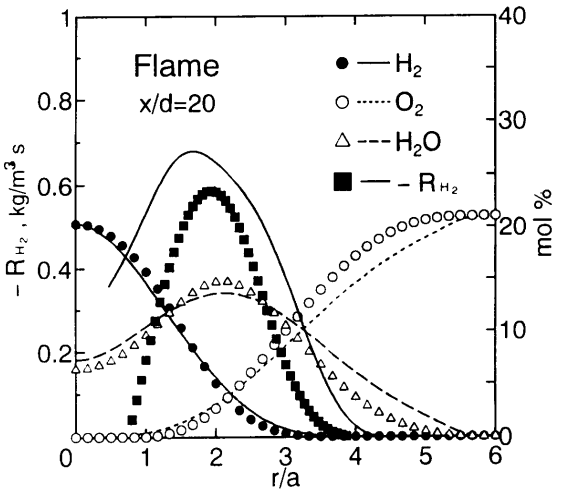

Fig. 7 Radial profiles of local reaction rate of H_2 and concentrations of H_2, O_2, and H_2O on the cross section of $x/d=20$. Plot is conducted with the experimental data by using Method A and line shows the simulation results.

results, precise agreement is observed in the correlation between the profiles of the local reaction rates and the coexistence manner of H_2 and O_2. This good agreement suggests that the method developed in the present study has a good performance to give the reliable values for local reaction rates.

6. Conclusions

It is desirable that local reaction rates are experimentally obtained when we estimate a modeling method for a turbulent combustion field by comparing the simulated results with experimental data. In the present study, a method was developed to calculate numerically local reaction rates and effective diffusion coefficients using experimental data for a hydrogen jet diffusion flame. Simultaneously, numerical simulation was conducted for that flame and the simulated local reaction rates and the diffusion coefficients were compared with the foregoing experimental ones. The conclusions are as follows.

(1) The calculation method developed in the present study was found to derive reliable values of local reaction rates from experimental data.

(2) It was suggested that the conserved scalar approach under the assumption of one-step irreversible reaction with fast chemistry can predict reliable local reaction rates for hydrogen jet diffusion flames.

(3) Though it is difficult to estimate correctly the derived diffusion coefficients, it was seen to correspond qualitatively to the simulated results.

The present study is a first step for the development of a method to obtain experimentally local reaction rates. Therefore, hydrogen was used as fuel for reasons of its simple reaction and stable combustion. However, since hydrogen has a large molecular diffusivity, a problem may possibly happen in the assumption that effective diffusion coefficients are the same for all chemical species. The study in that the fuel is changed to carbon monoxide is planned to clarify this question.

References

(1) Senecal, J. A. and Shipman, C. W., 17th Symp. (Int.) on Comb., (1979), p. 355.

(2) Vranos, A., et al., 12th Symp. (Int.) on Comb., (1969), p. 1051.

(3) Takagi, T., Okamoto, T., Taji, M., Nakasuji, Y. and Kondoh, T., Trans. Jpn. Soc. Mech. Eng., (in Japanese), Vol. 53, No. 488, B(1987), p. 1418.

(4) Lockwood, F. C. and Naguib, A. S., Combust. Flame, Vol. 24(1975), p. 109.